Bioconjugate Chemistry

pubs.acs.org/bc

Article

Colistin Crosslinked Gemcitabine Micelles to Eliminate Tumor Drug Resistance Caused by Intratumoral Microorganisms

Qian Qiu, Di Lu, Gengqi Liu, Xingyue Yang, Jiexin Li, He Ren, Jingang Liu, Boyang Sun, and Yumiao Zhang*

Cite This: *Bioconjugate Chem.* 2022, 33, 1944−1952

Read Online

ACCESS | Metrics & More | Article Recommendations | Supporting Information

ABSTRACT: In the tumor microenvironment, there exist microorganisms that metabolize anticancer drugs, leading to chemotherapy failure. To solve this problem, herein, we develop antibiotic and anticancer drug co-delivery micelles, termed colistin crosslinked gemcitabine micelle (CCGM). A self-immolative linker enables colistin and gemcitabine to be released on demand without affecting their antibacterial and anticancer effects. Once CCGM is delivered to the tumor microenvironment, intracellular glutathione triggers the release of colistin and gemcitabine, inhibiting the growth of microbes in the tumor, thus eliminating the microbe-induced drug resistance of tumor.

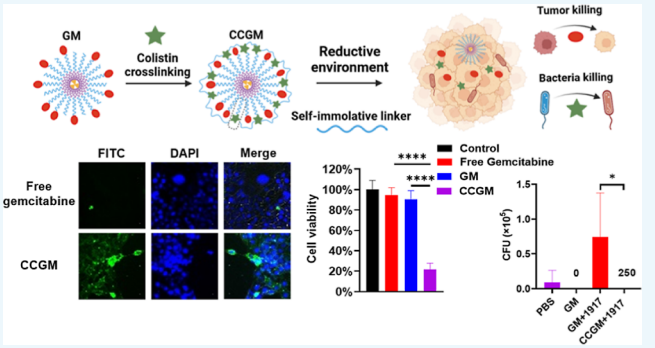

INTRODUCTION

Cancer is one of the leading causes of human death.[1] Although great achievements have been made in tumor treatments including surgery, radiation therapy, chemotherapy, immunotherapy, and drug resistance still exist as an important reason for treatment failure.[2−6] There are many mechanisms of tumor resistance, such as drug inactivation, drug target alteration, drug efflux, DNA damage repair, cell death inhibition, and tumor heterogeneity.[7−12] It was also found that microbes in tumors can cause tumors to develop drug resistance.[13]

Microorganisms abundantly exist in the human body, and some microorganisms can also affect the growth of tumors.[14−16] It was shown that there are various microorganisms in tumors, and they are specific in different types of tumors.[17−22] For example, there are many Proteobacteria in pancreatic cancer, while the microbes in colorectal cancer are mostly phylum Firmicutes and Proteobacteria.[23] The sources of microbes in tumors could be either native microbes in the tumor tissue or exogenous microbes from other tissues.[24−26] Microbes in gut and oral are also the sources of tumor microbes, and *Escherichia coli* in the intestine can enter the tumor through the circulatory system, indicating that the gut microbiota may have an impact on the types of microbes in the tumors.[25] Some intestinal microbes can metabolize chemotherapy drugs, such as doxorubicin.[27] In addition, the Gammaproteobacteria with the cytidine deaminase gene can metabolize gemcitabine into its inactive form of 2′,2′-difluorodeoxyuridine, making it ineffective for tumor treatment.[13]

Gemcitabine, a cytidine anticancer drug approved by the FDA as a first-line anticancer drug in 1996,[28] has been widely used for the treatment of various solid tumors.[29−33] Gemcitabine has poor stability and can be metabolically inactivated by cytidine deaminase in the blood and kidneys.[34] To address this problem, various gemcitabine prodrugs and carriers have been developed, but tumor resistance to gemcitabine still not well solved.[35] Gammaproteobacteria existing in tumor tissue could uptake gemcitabine prodrugs or its nanoformulations and make them metabolically inactive. Recently, Xi et al. developed a nanoenzyme system to inhibit the activity of cytidine deaminase and eliminate the tumor resistance caused by microorganisms.[36] In addition, altering the microbial composition in the tumor microenvironment or inhibiting its growth using antibiotics is also a feasible approach.

In this study, we designed a co-delivery micelle of colistin and gemcitabine to eliminate bacteria-induced cancer resistance. The gemcitabine chemically linked with a self-immolative linker was conjugated to Pluronic F127 to prepare the gemcitabine-F127 polymer (G-F127); then, colistin, a potent amine-containing antibiotic, was used as a crosslinker to make colistin-crosslinked gemcitabine-F127 micelles (CCGM).[37,38] Once CCGM reaches the tumor tissue containing bacteria, the reductive environment enables the rapid release of gemcitabine and colistin, inhibiting bacterial growth and simultaneously

Received: August 31, 2022
Revised: September 21, 2022
Published: October 3, 2022

treating the tumor, avoiding the gemcitabine metabolism induced by intratumor bacteria.[39]

RESULTS AND DISCUSSION

Co-delivery of Gemcitabine and Colistin. In order to prepare gemcitabine-conjugated F127 (G-F127), the hydroxyl groups on F127 were first chemically converted to thiols, and gemcitabine was then conjugated to the resulting F127-SH via a self-immolative linker. The synthetic routes of linker, conversion of F127 to F127-SH, and the conjugation of gemcitabine are illustrated in Figures S1−S4. The amine-reactive self-immolative linker was mixed with G-F127 with the molar ratio of approximately 1 (linker):1 (gemcitabine on G-F127) (Figure S5), so the remaining amine-reactive sites on the surface of micelles could be crosslinked by colistin. To enhance the micelle stability, an extremely hydrophobic coenzyme Q10 (CoQ10) was encapsulated in the core of G-F127 micelles (denoted as GM without colistin crosslinking as a control). Then, colistin was used as an antibiotic for bacterial killing and a crosslinker for crosslinking GM. In addition, the resulting colistin-crosslinked GM was termed CCGM. As shown in Figure 1, due to the

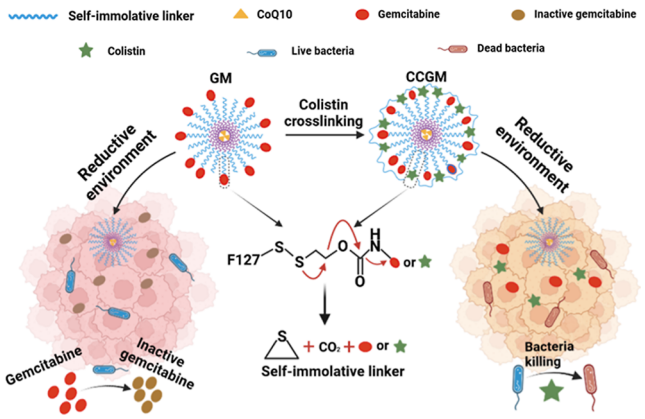

Figure 1. Schematic illustration of CCGM eliminating bacteria-induced cancer drug resistance.

presence of *E. coli* Nissle 1917, gemcitabine was rapidly metabolized and inactivated. After CCGM was delivered to the tumor, the reductive environment caused the rapid release of colistin and killed the bacteria, thereby eliminating the bacteria-induced cancer drug resistance.

Characterization of CCGM. As shown in Figure 2A, the presence of CoQ10 in the core and the crosslinking of colistin both enhanced the yield of gemcitabine in CCGM. Multiple amine groups on colistin could react with the remaining linkers on GM, which further improved the yield of micelles. As shown in Figure 2B, owing to colistin crosslinking, the surface charge of CCGM was converted to positive because of the amine groups on colistin, which could enhance the cellular uptake due to the electrostatic interaction between CCGM and the cell membrane. The size of the CCGM was about 189.6 ± 2.8 nm measured by dynamic light scattering analysis (Figure 2C). The spherical morphology of CCGM was visualized by a transmission electron microscope with negatively staining by a 1% uranyl acetate aqueous solution, as shown in Figure 2D. Then, the release of gemcitabine from CCGM was also investigated. As shown in Figure 2E, gemcitabine was almost completely released within 4 h when incubation with 10 mM tris(2-carboxyethyl)-phosphine (TCEP), whereas there was almost no release in PBS. Similar to our previous findings, drugs on CCGM could be rapidly released in a reductive environment, owing to the self-immolative linker and the self-immolation process was proposed in Figure 1.[40]

Effects of Bacteria on Gemcitabine. To study the effect of Gammaproteobacteria on gemcitabine, *E. coli* Nissle 1917 was chosen and incubated with gemcitabine, and the properties of gemcitabine were characterized by HPLC and an ultraviolet−visible spectrophotometer. As shown in Figure 3A, the retention time of gemcitabine changed from 3.9 to 4.9 min after incubation with *E. coli* Nissle 1917, which indicated that gemcitabine was likely to be metabolized by bacteria. Figures 3B and S6 show the kinetics of gemcitabine metabolism in the presence of bacteria. In addition, the absorbance spectra were compared when gemcitabine was incubated in the culture medium with or without bacteria for 3 h. As shown in Figure 3C, after incubation in the culture medium without bacteria, the characteristic peaks remained the same as that of gemcitabine aqueous solution. However, with bacteria, the characteristic peak blue-shifted from 268 to 258 nm. Presumably, bacteria with genes encoding cytidine deaminase naturally or exogenously existing in tumor tissue could cause drug resistance of tumors. In addition, bacteria with genes encoding cytidine deaminase can metabolize gemcitabine into its inactive form, 2′,2′-difluorodeoxyuridine. Free gemcitabine, GM, and CCGM were incubated with *E. coli* Nissle 1917 to study the protective effect of micelles on gemcitabine. As shown in Figure 3D, after incubation with *E. coli* Nissle 1917, the retention of drug in free gemcitabine was minimal due to the metabolism of drug by bacteria. Also, both the micellar forms of GM and CCGM have shown protective effects against gemcitabine, especially CCGM exhibited the highest retention and best protective effect due to the antimicrobial effect of colistin.

Cellular Uptake. Next, we investigated in vitro cellular uptake of CCGM. Free gemcitabine, GM, and CCGM were incubated with 4T1 cells for 4 h. TX-100 and TCEP were used for cell lysis and the release of gemcitabine, respectively. Cellular uptake of gemcitabine was quantified by HPLC. As shown in Figure 4A, CCGM exhibited the highest cellular uptake, approximately twice than that of free gemcitabine. The cellular uptake of GM was higher than that of free gemcitabine because of the hydrophobicity of linker-modified micelles, and the positive charge of CCGM imparted by colistin that further enhanced the cellular uptake. Then, fluorescein isothiocyanate (FITC)-labeled gemcitabine was used to prepare micelles for cellular uptake quantification. As shown in Figure S7, the difference between fluorescence spectra before and after FITC labeling suggested that FITC was successfully labeled on gemcitabine. FITC-gemcitabine, FITC-GM, and FITC-CCGM were incubated with 4T1 cells for 4 h, and then cells were collected and analyzed by flow cytometry. As shown in Figure 4B, FITC-CCGM exhibited the highest fluorescence signal, similar to the results in Figure 4A. Fluorescence microscopic images of cells taking up free gemcitabine, GM, and CCGM provided a similar trend of cellular uptake of different formulations (Figure 4C).

Antibacterial and Anticancer Ability In Vitro. To evaluate the anticancer efficacy of CCGM, different formulations including free gemcitabine, GM, and CCGM were incubated with 4T1 cells for 24 h, and then the anticancer effect was assessed using the CCK-8 viability assay. As shown in Figure 5A, cell viability decreased with increasing gemcitabine concentration. When the concentration of gemcitabine reached

https://doi.org/10.1021/acs.bioconjchem.2c00407
Bioconjugate Chem. 2022, 33, 1944−1952

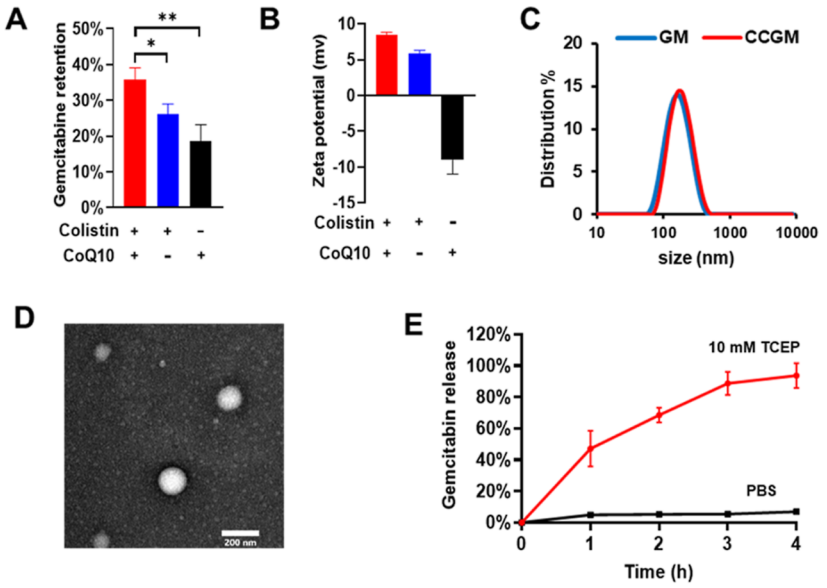

Figure 2. Characterization of CCGM. (A) Enhanced yield of CCGM due to the stabilization of CoQ10 and colistin crosslinking. (B) Effects of CoQ10 and colistin on the ζ-potential. (C) Size of GM and CCGM. (D) Transmission electron microscopic images of CCGM. Scale bar: 200 nm. (E) Gemcitabine release from CCGM in the presence of PBS or 10 mM TCEP. *$p < 0.05$, **$p < 0.01$, and ***$p < 0.001$, as analyzed by one-way ANOVA, followed by Bonferroni's post hoc analysis ($n = 3$; data are means ± SD).

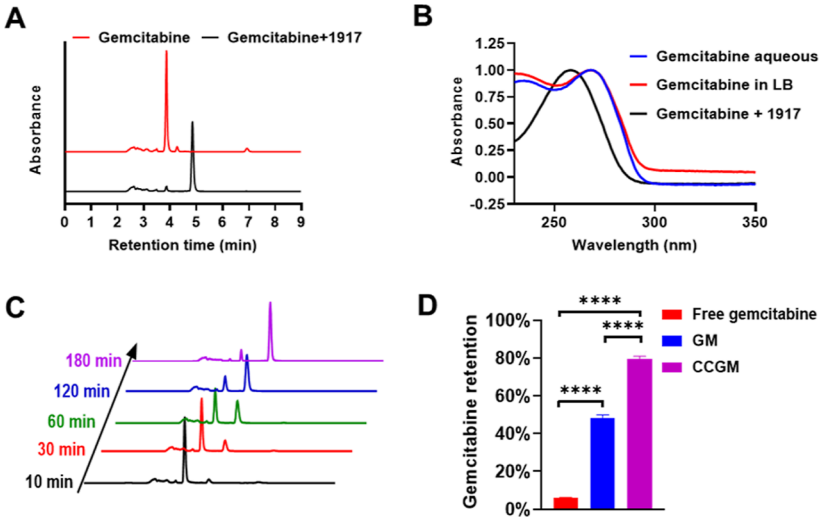

Figure 3. Effects of bacteria on gemcitabine. (A) HPLC characteristic peaks of gemcitabine before and after being metabolized. (B) Metabolism of gemcitabine over time. (C) Gemcitabine before and after being metabolized and detected by UV−vis. (D) Protective effect of GM and CCGM on gemcitabine ($n = 3$; data are means ± SD). *$p < 0.05$, **$p < 0.01$, ***$p < 0.001$, and ****$p < 0.0001$, as analyzed by one-way ANOVA, followed by Bonferroni's post hoc analysis.

5 or 10 μg/mL, the anticancer effect of GM and CCGM was higher than that of free gemcitabine probably because of higher cellular uptake. In addition, to evaluate the antimicrobial efficacy of CCGM, the minimum inhibitory concentrations (MICs) were measured with or without glutathione (GSH) against *E. coli* Nissle 1917 by the checkerboard dilution method. Additionally, the IC_{50} values of free gemcitabine, GM, and CCGM were calculated to be 8.115, 5.767, and 5.463 μg/mL, respectively (Figure S8). As shown in Figure 5C, the MIC of CCGM + GSH was about 8 μg/mL, similar to the MIC of free colistin. The MIC of CCGM without GSH was about 16 μg/mL, which was twice as high as CCGM with GSH because some of the amine groups on the colistin were masked by a self-immolative linker, without restoring the antimicrobial effect of colistin.

Then, 4T1 cells were cultured with bacteria and incubated with free gemcitabine, GM, and CCGM for 24 h respectively, and then cell viability was assessed using the CCK-8 viability assay. As shown in Figure 5B, free gemcitabine and GM groups exhibited almost no anticancer activity, while CCGM exhibited strong anticancer activity. Due to the antibacterial effect of colistin, the growth of bacteria in the medium of the CCGM group was inhibited, while gemcitabine in free gemcitabine and GM groups was metabolized by bacteria and thus did not exhibit anticancer effects.

In Vivo Antitumor Efficacy. Encouraged by the in vitro anticancer efficacy of CCGM, we next evaluated the in vivo anticancer efficacy of CCGM on drug-resistant tumors. Murine drug-resistant tumor model was established by intravenously injecting *E. coli* Nissle 1917 that could colonize the tumor tissue

https://doi.org/10.1021/acs.bioconjchem.2c00407
Bioconjugate Chem. 2022, 33, 1944−1952

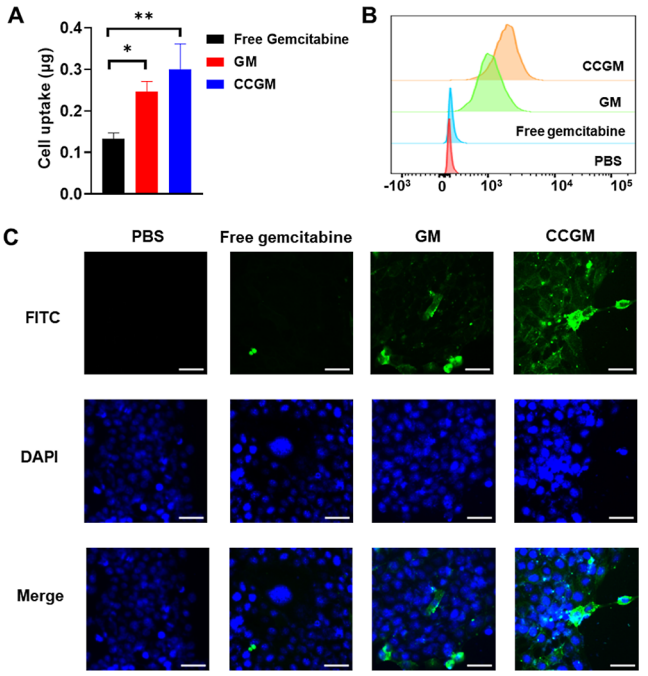

Figure 4. Cellular uptake. (A) Cellular uptake of free gemcitabine, GM, and CCGM, and gemcitabine was FITC labeled (n = 3; data are means ± SD). (B) Cellular uptake analyzed by flow cytometry. (C) Fluorescence microscope image. Scale bar = 50 μm. *p < 0.05, **p < 0.01, and ***p < 0.001, as analyzed by one-way ANOVA, followed by Bonferroni's post hoc analysis.

in mice. Briefly, mice were randomly divided into six groups (n = 6): (I) intravenous (i.v.) injection of PBS plus i.v. injection of *E. coli* Nissle 1917, (II) i.v. injection of GM plus i.v. injection of *E. coli* Nissle 1917, (III) i.v. injection of CCGM plus i.v. injection of *E. coli* Nissle 1917, (IV) i.v. injection of PBS, (V) i.v. injection of GM, and (VI) i.v. injection of CCGM (Figure 6A). Compared with I and II groups, the tumors in the III group were effectively suppressed (Figure 6B), and a 100% survival rate was achieved after 20 days (Figure 6D). This was due to the bacteria colonized in the tumor-metabolized gemcitabine, whereas the colistin on the CCGM inhibited the growth of bacteria, so that drug resistance was eliminated, leading to the recovery of anticancer efficacy of gemcitabine. Compared with V and VI groups, III group also showed comparable antitumor efficiency, further validating the effectiveness of the colistin crosslinking strategy (Figure 6B). To demonstrate the antibacterial effect of CCGM in vivo, we also calculated the CFU number of tumors in each group. As shown in Figures 6E and S9, the CCGM + 1917 group almost had no bacteria, similar to the PBS and GM groups. In contrast, the CFUs of bacteria in the GM + 1917 group was about 300 times higher than that of the CCGM + 1917 group. This showed that CCGM could effectively eliminate the tumor resistance caused by intratumor bacteria. As shown in Figure 6C, the body weights of mice in the CCGM-treated group did not exhibit any abnormality, indicating the good biosafety of CCGM. In order to further evaluate the safety profile of CCGM, pharmacokinetics and biodistribution were also assessed. As demonstrated in Figure S10, the GM and CCGM exhibited relative long circulation time in blood and did not get quickly cleared by serum. To visualize the distribution of gemcitabine in tissues, gemcitabine was fluorescently labeled by FITC first, and different formulations were injected intravenously in mice, followed by imaging of organs under a fluorescence microscope. Compared with free gemcitabine, GM and CCGM were accumulated more in the liver (Figure 6F). Also, as shown in Figure S11, significant accumulation of the drug in the tumor was also observed likely owing to the enhanced permeability and retention effect. Furthermore, tumor slices collected from I to VI group mice were stained with terminal deoxynucleotidyl transferase dUTP nick-end labeling

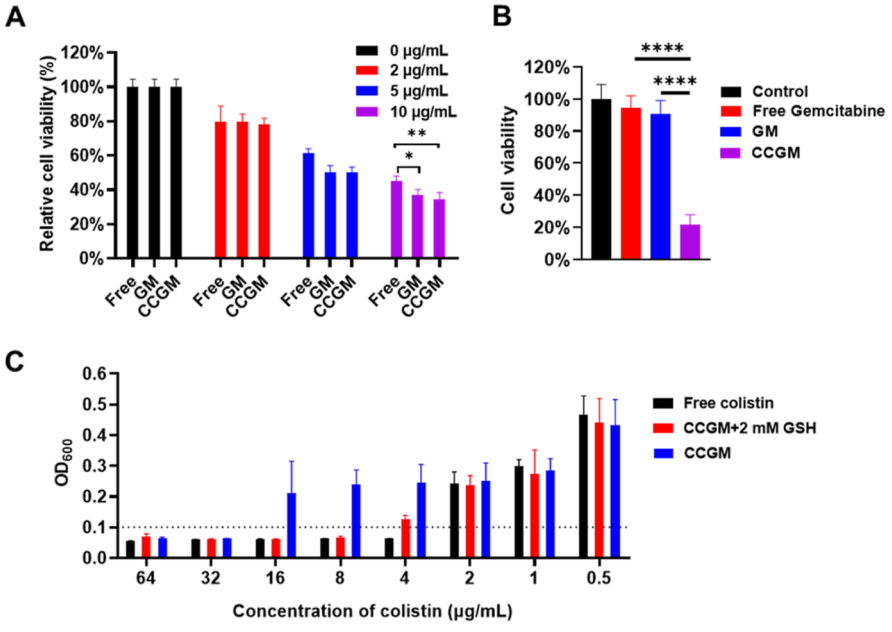

Figure 5. Antibacterial and anticancer ability in vitro. (A) Anticancer efficacy of free gemcitabine, GM, and CCGM in vitro (n = 5; data are means ± SD). (B) In vitro anticancer effects of free gemcitabine, GM, and CCGM in the presence of bacteria (n = 5; data are means ± SD). The concentration of each drug is 35 μg/mL. (C) MIC determination of free colistin and CCGM with or without GSH (n = 3; data are means ± SD). *p < 0.05, **p < 0.01, ***p < 0.001, and ****p < 0.0001, as analyzed by one-way ANOVA, followed by Bonferroni's post hoc analysis.

https://doi.org/10.1021/acs.bioconjchem.2c00407
Bioconjugate Chem. 2022, 33, 1944−1952

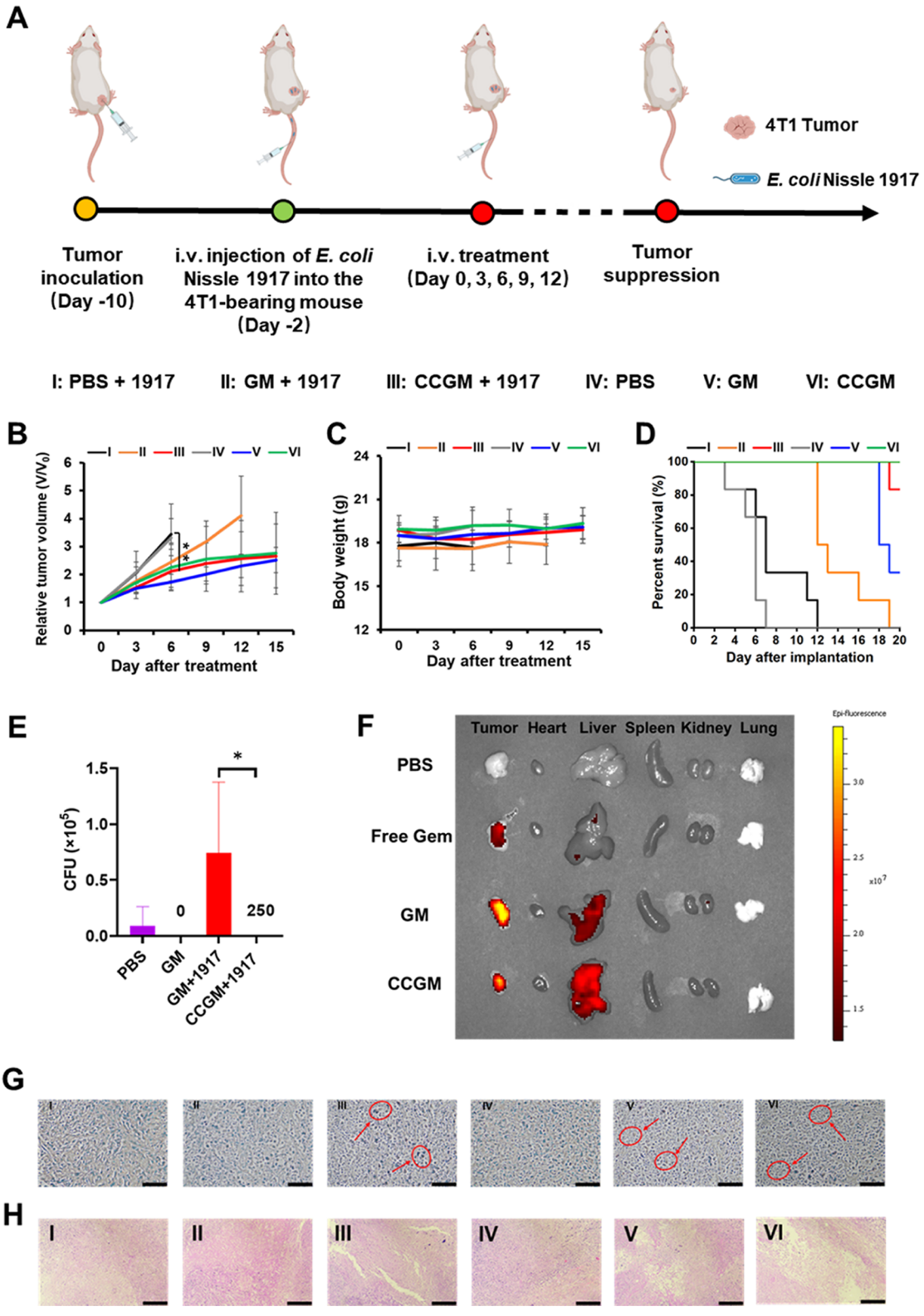

Figure 6. CCGM-enhanced anticancer activity of Gem in the mouse model of subcutaneous breast cancer with intratumor *E. coli* Nissle 1917. Data are means ± SD ($n = 6$). (A) Treatment schedule. Subcutaneous model of breast cancer (4T1) was established in Balb/c mice. *E. coli* Nissle 1917 bacteria were injected i.v. and selectively colonized in tumors. (B) Tumor growth curves of different groups after GM and CCGM treatment. (C) Body weight changes in mice after different treatments. (D) Survival of mice after different treatments. (E) CFUs of tumor homogenate. (PBS group: $n = 3$, other groups: $n = 4$; data are means ± SD) $^*p < 0.05$, $^{**}p < 0.01$, and $^{***}p < 0.001$, as analyzed by one-way ANOVA, followed by Bonferroni's post hoc analysis. (F) The biodistribution 24 h after mice was intravenous injection of PBS, free gemcitabine, GM, and CCGM. Fluorescence imaging of tumor and organs including heart, liver, spleen, kidney, and lung after mice were given FITC-labeled free gemcitabine, GM, and CCGM and sacrificed at 24 h. (G,H) TUNEL and H&E staining of dissected tumor tissues. Scale bar = 100 μm. (I) PBS + 1917, (II) GM + 1917, (III) CCGM + 1917, (IV) PBS, (V) GM, and (VI) CCGM.

https://doi.org/10.1021/acs.bioconjchem.2c00407
Bioconjugate Chem. 2022, 33, 1944−1952

(TUNEL). Compared with the control group, the III, V, and VI groups had more tumor cells with brown color (highlighted by circles and arrows), indicative of apparent cell apoptosis (Figure 6G). The comparison of the II and III groups revealed the bactericidal effect of colistin. Also, hematoxylin and eosin (H&E) staining images were also taken, and images of tumors collected from III, V, and VI groups exhibited histological structures with loose tissue gaps and reduced number of tumor cells (Figure 6H).

Biocompatibility Evaluation of CCGM. Finally, the biocompatibility of CCGM was assessed in CD-1 mice. The mice were divided into two groups; PBS or 4 mg kg^{-1} CCGM was intravenously administered to mice via tail vein injection every 3 days for a total of five injections. After 24 h of the last injection, bloods and organs were collected for complete blood count (CBC) analysis and H&E analysis. As shown in Figure S12, there was no significant difference for the CBC parameters as indicated between mice given PBS or CCGM including red blood cell count, platelet count, neutrophil (Neu) count, mean cell volume, and others. Major organs collected from mice treated with PBS and CCGM were examined by H&E staining analysis, and no inflammation or other overt abnormality was observed (Figure S13). These data indicate that CCGM appears to be favorably biocompatible without causing acute toxicity following i.v. injection, at least in mice.

CONCLUSIONS

In summary, we synthesized a gemcitabine and colistin co-delivery micellar system using colistin as a crosslinker to enhance the micelle stability and importantly to eliminate bacteria-induced drug resistance of tumor. Colistin and gemcitabine were linked to micelles by a self-immolative linker, and they could be released in response to the reducing environment in tumors. In vitro and in vivo results collectively showed that CCGM had good antibacterial and anticancer effects, effectively preventing gemcitabine from being metabolized by intratumor bacteria. Altogether, CCGM, as a new biomaterial, shows great promise for the elimination of drug resistance and enhanced antitumor efficacy for microbe-induced drug-resistant tumor treatment.

EXPERIMENTAL SECTION

Materials and Reagents. Pluronic F127 and CoQ10 were purchased from Sigma-Aldrich. Gemcitabine hydrochloride was purchased from Shanghai Dibo Biotechnology Co., Ltd. 4-Dimethylaminopyridine (DMAP) and colistin sulfate salt (colistin) were purchased from Shanghai Yuanye Bio-Technology Co., Ltd. FITC, *N*,*N*-diisopropylethylamine (DIPEA), and TCEP were purchased from Heowns Biochem Technologies, LLC, Tianjin. *N*,*N*-Dimethylformamide (DMF) was purchased from Tianjin Bohai Chemical Industry Group Co., Ltd. Dichloromethane was purchased from Tianjin Jiangtian Chemical Technology Co., Ltd. Dimethyl sulfoxide (DMSO) was purchased from Tianjin Kemiou Chemical Reagent Co., Ltd. *E. coli* Nissle 1917 was purchased from Beijing Biobw Biotechnology Co., Ltd. 4T1 cells were kindly provided by Prof. Xiaoli Wang's group. Balb/c and CD-1 mice were purchased from Charles River Beijing Co., Ltd.

Synthesis of G-F127 (Gemcitabine-Conjugated Pluronic F127). G-F127 was made by conjugating gemcitabine to Pluronic F127 (F127) via a self-immolative linker. Sulfhydryl Pluronic F127 (SH-F127) and self-immolative linker were first synthesized as previously reported.[40,41] Gemcitabine was first chemically modified by the self-immolative linker by dissolving 0.05 mmol of self-immolative linker and 0.05 mmol of gemcitabine hydrochloride in 1 mL of DMF, and 12 μL of DIPEA and 0.01 mmoL of DMAP were added in the DMF solution above and stirred for 16 h. Then, 0.02 mmoL SH-F127 was dissolved in 20 mL of dichloromethane, followed by adding the above DMF solution dropwise in it and stirring for overnight. Then, dichloromethane was evaporated under vacuum, the mixture was dissolved in H_2O and dialyzed with a 8000−14 000 MWCO dialysis bag, and the final product of G-F127 was collected after freeze-drying.

Preparation of GM and CCGM. G-F127 micelles (GM) were made as a control without colistin crosslinking by using CoQ10 in the core of micelles for stabilization. Briefly, CoQ10 (0.6 mg) dissolved in 100 μL of dithiothreitol was added to 1 mL of 5% (wt %) G-F127 aqueous solution, followed by stirring for 2 h. To further make colistin crosslinked GM (CCGM), 5 mg of colistin in 100 μL of distilled water was added to the above G-F127 solution, and then 5 μL of 1 mol/L NaOH aqueous solution was added to adjust the pH value for crosslinking and then stirred for 2 h. The final solution was centrifuged in a centrifugal filtration device with an ultrafiltration centrifugal tube three times to remove free colistin and unstable micelles.

Characterization of GM and CCGM. To investigate the effects of CoQ10 and colistin on micelle stability, different control formulations were made. Briefly, 0.6 mg of CoQ10 + 5 mg of colistin, 5 mg of colistin with no CoQ10, and 0.6 mg of CoQ10 with no colistin were added, and the other steps were the same as described before. To study the release of gemcitabine, 10 mM TCEP was added to the gemcitabine micelles formulations as indicated in Figure 2E, and the released drug was detected by HPLC (Agilent 1260 Infinity II). The size and ζ potential were measured by a nanoparticle size and ζ potential analyzer (Nano ZS, Malvern). The morphology of CCGM was observed by a transmission electron microscope (JEM-1400Flash) after negatively staining by 1% uranyl acetate. The release activity of CCGM was measured under reductive conditions (10 mM TCEP) and PBS at 37 °C, and the release of gemcitabine was measured by HPLC. The mobile phase of HPLC consisted of 90% sodium acetate buffer with pH = 4.6 and 10% acetonitrile on the rate of 0.5 mL/min, and gemcitabine was detected at 267 nm.

Effect of Bacteria on Gemcitabine In Vitro. *E. coli* Nissle 1917 (1917) was cultured with LB liquid medium overnight in a constant-temperature shaker (37 °C, 180 rpm), 1 mg of gemcitabine was added in 1 mL LB liquid medium with bacteria, a part of the solution was taken out at a specific time as indicated, and the characteristic peaks of gemcitabine were detected by HPLC and a ultraviolet−visible spectrophotometer (Thermo Scientific).

To study the protective effect of GM and CCGM on gemcitabine, free gemcitabine, GM, and CCGM were added to fresh bacterial culture medium, followed by the addition of 10 μL of *E. coli* Nissle 1917 culture medium and incubated at 37 °C, 180 rpm for 8 h. After that, the bacteria were removed by centrifugation, the supernatant was diluted 10-fold with TCEP solution and incubated overnight at 37 °C, and the gemcitabine concentration was quantified by HPLC.

Cellular Uptake and Intracellular Distribution. To study the cellular uptake, 1×10^6 4T1 cells were transferred to six-well plates and incubated overnight at 37 °C with 5% CO_2. Subsequently, the cells were incubated with free gemcitabine, GM, and CCGM in medium for 4 h. Then, the medium was

https://doi.org/10.1021/acs.bioconjchem.2c00407
Bioconjugate Chem. 2022, 33, 1944−1952

removed and washed with PBS three times. After that, cells were lysed by 1% Triton X-100 (TX-100), and TCEP was added to release gemcitabine on micelles. Gemcitabine uptake into cells was quantified by HPLC.

To visualize the effect of cellular uptake, FITC-labeled gemcitabine was used to prepare FITC-GM and FITC-CCGM. To label gemcitabine with FITC, 0.1 mmol gemcitabine hydrochloride was dissolved in 3 mL of ultrapure water, the pH value was adjusted to 10 with NaOH, and then 0.01 mmol FITC in 300 μL of DMSO was added to it and stirred for 4 h. Then, the solution was lyophilized. The other steps for preparing GM and CCGM were similar as described before. 1×10^6 4T1 cells were transferred to six-well plates overnight and then incubated with free FITC-gemcitabine, FITC-GM, and FITC-CCGM in medium for 4 h. Cells were washed three times by PBS, resuspended, and analyzed by flow cytometry (FACSAria III, BD). For the intracellular distribution study, cells were washed with PBS and stained with DAPI and then were observed by a fluorescence microscope (Nikon ECLIPSE ti2).

In Vitro Anticancer and Antibacterial Efficacy of CCGM. For the in vitro anticancer study, 5×10^4 4T1 cells were transferred to 96-well plates and incubated overnight, and then the medium was replaced with a fresh medium with free gemcitabine, GM, or CCGM in different concentrations (1, 2, and 5 μg/mL) and incubated for 24 h. Then, the medium was removed, the cells were washed with PBS three times, and the cell viability was detected by the CCK-8 kit.

MIC was measured to study the antibacterial ability of CCGM. For colistin quantification, we prepared CCMG with FITC-labeled colistin.[42] *E. coli* Nissle 1917 was cultured to logarithmic phase in the LB liquid medium, and the bacteria were diluted 100-folds with PBS. Then, free colistin or CCGM (with 2 mM GSH) or CCGM (without GSH) dissolved in the Mueller−Hinton broth medium were placed in 96-well plates with different concentrations, the concentration range of colistin was 64−0.5 μg/mL by the broth microdilution method, and 20 μL of bacteria PBS solution was added and incubated overnight. The absorbance of each well at 600 nm was measured by a microplate reader (Infinite M Nano$^+$).

To study the ability of CCGM to eliminate the drug resistance of 4T1 cells caused by bacteria, 5×10^4 cells were transferred to 96-well plates overnight, and then the medium was replaced by the medium with *E. coli* Nissle 1917. Free gemcitabine, GM, or CCGM was added in the medium to make the concentration of gemcitabine 35 μg/mL, followed by incubation for 24 h. After that, the medium was removed and washed 3 times with PBS. The cell viability was measured with the CCK-8 (Solarbio, Beijing, China) method.

Ability of CCGM to Eliminate Drug Resistance Caused by Bacteria In Vivo. Drug-resistant tumor models were prepared as previously reported.[13] Mice were purchased from Charles River Beijing Co., Ltd. (Beijing, China). Animal experiments were performed in accordance with the Tianjin University Institutional Animal Care and Use Committee (protocol number: TJUE-2020-033). Female Balb/c mice of age 6−8 weeks were subcutaneously injected with 1×10^6 4T1 cells. After about 1 week, the mice were randomly divided into six groups. Three groups were prepared as drug-resistant tumor models; *E. coli* Nissle 1917 were grown overnight at 37 °C and then diluted 100-folds with fresh media until growing to OD_{600} = 0.5. To evaluate the bacteria killing efficiency of CCGM, the bacteria were washed with PBS three times and diluted to 5×10^7 bacteria/mL, and each mice were injected 100 μL through the tail vein. For the normal tumor models, mice were injected 100 μL of sterile PBS. For normal tumor model mice, PBS or GM at a dose of 4.0 mg kg^{-1} gemcitabine was injected every 3 days for a total of five injections. For drug-resistant tumor models, GM or CCGM at a dose of 4.0 mg kg^{-1} gemcitabine was injected every 3 days. Tumor size and body weight were measured every day. After 20 days, the mice were sacrificed, and tumors were homogenized. The tissue homogenate of tumor was spread on bacteria culture dishes to count bacteria in tumors. TUNEL and H&E-stained sections were prepared by Tianjin Haosi Biotechnology Co., Ltd.

Pharmacokinetics and Biodistribution of CCGM. To determine half-life in blood and biodistributions in major organs, free gemcitabine, GM, and CCGM with a dose of 4 mg (gemcitabine) kg^{-1} were injected intravenously vial tail vein. The blood was collected at indicated time points. To prepare samples for analysis, 50 μL of serum and 300 μL of acetonitrile were mixed. The supernatant solution (350 μL) was collected after centrifugation at 8000 rpm for 10 min. The solvent was incubated with 3.5 μL of 2 M TCEP overnight before the HPLC assay. For fluorescence imaging of organs, mice are intravenously given FITC-labeled free gemcitabine, FITC-GM, and FITC-CCGM with 4 mg (gemcitabine) kg^{-1} gemcitabine. After 24 h of injection, mice were sacrificed and organs were collected and then imaged by IVIS (Night OWL II LB 983, Berthold Technologies) with excitation/emission wavelengths at 485/520 nm.

Biosafety Assay of CCGM. In order to evaluate the potential toxicity of CCGM in vivo, free gemcitabine and CCGM were injected into CD-1 mice via tail vein (4 mg kg^{-1}) every 3 days for a total of five injections, and then blood routine was performed after 24 h of the last injection. At the same time, the main organs of mice (heart, liver, spleen, liver, and kidney) were collected for H&E staining.

Statistical Analysis. Data was analyzed with GraphPad Prism 8.0.2. Statistical significance was analyzed by one-way ANOVA, followed by Bonferroni's post hoc analysis. Data was considered statistically significant when $p < 0.05$. Values were reported as the average standard deviation with the sample size.

■ ASSOCIATED CONTENT

Supporting Information

The Supporting Information is available free of charge at https://pubs.acs.org/doi/10.1021/acs.bioconjchem.2c00407.

Synthesis routes of gemcitabine-F127 and NMR, degradation rate of gemcitabine in LB with *E. coli* Nissle 1917, and pictures of tumors and bacteria in tumor homogenate (PDF)

■ AUTHOR INFORMATION

Corresponding Author

Yumiao Zhang − *School of Chemical Engineering and Technology, Key Laboratory of Systems Bioengineering (Ministry of Education), Frontiers Science Center for Synthetic Biology (Ministry of Education), Tianjin University, Tianjin 300350, P. R. China;* orcid.org/0000-0002-6166-0470; Email: ymzhang88@tju.edu.cn

Authors

Qian Qiu − *School of Chemical Engineering and Technology, Key Laboratory of Systems Bioengineering (Ministry of Education), Frontiers Science Center for Synthetic Biology*

(Ministry of Education), Tianjin University, Tianjin 300350, P. R. China

Di Lu − *School of Chemical Engineering and Technology, Key Laboratory of Systems Bioengineering (Ministry of Education), Frontiers Science Center for Synthetic Biology (Ministry of Education), Tianjin University, Tianjin 300350, P. R. China*

Gengqi Liu − *School of Chemical Engineering and Technology, Key Laboratory of Systems Bioengineering (Ministry of Education), Frontiers Science Center for Synthetic Biology (Ministry of Education), Tianjin University, Tianjin 300350, P. R. China*

Xingyue Yang − *School of Chemical Engineering and Technology, Key Laboratory of Systems Bioengineering (Ministry of Education), Frontiers Science Center for Synthetic Biology (Ministry of Education), Tianjin University, Tianjin 300350, P. R. China*

Jiexin Li − *School of Chemical Engineering and Technology, Key Laboratory of Systems Bioengineering (Ministry of Education), Frontiers Science Center for Synthetic Biology (Ministry of Education), Tianjin University, Tianjin 300350, P. R. China*

He Ren − *School of Chemical Engineering and Technology, Key Laboratory of Systems Bioengineering (Ministry of Education), Frontiers Science Center for Synthetic Biology (Ministry of Education), Tianjin University, Tianjin 300350, P. R. China*

Jingang Liu − *School of Chemical Engineering and Technology, Key Laboratory of Systems Bioengineering (Ministry of Education), Frontiers Science Center for Synthetic Biology (Ministry of Education), Tianjin University, Tianjin 300350, P. R. China*

Boyang Sun − *School of Chemical Engineering and Technology, Key Laboratory of Systems Bioengineering (Ministry of Education), Frontiers Science Center for Synthetic Biology (Ministry of Education), Tianjin University, Tianjin 300350, P. R. China*

Complete contact information is available at: https://pubs.acs.org/10.1021/acs.bioconjchem.2c00407

Author Contributions

Q.Q., D.L., and G.L. contributed equally. Q.Q., Y.Z. conceived the project. Q.Q. and D.L. carried out most experiments. G.L. and J.L. assisted with chemical synthesis experiments. X.Y. and J.L. assisted with bacterial experiments. H.R. assisted with animal experiments. Q.Q., D.L., and Y.Z. performed data analysis and wrote the manuscript.

Funding

This work was supported by the National Natural Science Foundation of China (32071384), the National Key Research and Development Program (2021YFC2102300), the Start-up Grant at Tianjin University, and One-thousand Young Talent Program of China.

Notes

The authors declare no competing financial interest.

■ ACKNOWLEDGMENTS

We thank the funding sources mentioned in Funding Sources.

■ REFERENCES

(1) World Health Organization. *WHO Report on Cancer: Setting Priorities, Investing Wisely and Providing Care for All*, 2020.

(2) Zhang, C.; Zeng, Z.; Cui, D.; He, S.; Pu, K. Semiconducting polymer nano-PROTACs for activatable photo-immunometabolic cancer therapy. *Nat. Commun.* **2021**, *12*, 2934.

(3) Plesca, M.; Bordea, C.; El Houcheimi, B.; Ichim, E.; Blidaru, A. Evolution of radical mastectomy for breast cancer. *J. Med. Life* **2016**, *9*, 183.

(4) DeVita, V. T.; Chu, E. A history of cancer chemotherapy. *Cancer Res.* **2008**, *68*, 8643−8653.

(5) Dobosz, P.; Dzieciątkowski, T. The intriguing history of cancer immunotherapy. *Front. Immunol.* **2019**, *10*, 2965.

(6) Mansoori, B.; Mohammadi, A.; Davudian, S.; Shirjang, S.; Baradaran, B. The different mechanisms of cancer drug resistance: a brief review. *Adv. Pharm. Bull.* **2017**, *7*, 339.

(7) Mehta, K.; Fok, J. Y. Targeting transglutaminase-2 to overcome chemoresistance in cancer cells. In *Drug Resistance in Cancer Cells*; Springer, 2009; pp 95−114.

(8) Friche, E.; Danks, M. K.; Schmidt, C. A.; Beck, W. T. Decreased DNA topoisomerase II in daunorubicin-resistant Ehrlich ascites tumor cells. *Cancer Res.* **1991**, *51*, 4213−4218.

(9) Gottesman, M. M.; Fojo, T.; Bates, S. E. Multidrug resistance in cancer: role of ATP−dependent transporters. *Nat. Rev. Cancer* **2002**, *2*, 48−58.

(10) Ricci, M. S.; Zong, W.-X. Chemotherapeutic approaches for targeting cell death pathways. *Oncologist* **2006**, *11*, 342−357.

(11) Turner, K. M.; Deshpande, V.; Beyter, D.; Koga, T.; Rusert, J.; Lee, C.; Li, B.; Arden, K.; Ren, B.; Nathanson, D. A. Extrachromosomal oncogene amplification drives tumour evolution and genetic heterogeneity. *Nature* **2017**, *543*, 122−125.

(12) Gao, Z.; Zhang, L.; Sun, Y. Nanotechnology applied to overcome tumor drug resistance. *J. Controlled Release* **2012**, *162*, 45−55.

(13) Geller, L. T.; Barzily-Rokni, M.; Danino, T.; Jonas, O. H.; Shental, N.; Nejman, D.; Gavert, N.; Zwang, Y.; Cooper, Z. A.; Shee, K. Potential role of intratumor bacteria in mediating tumor resistance to the chemotherapeutic drug gemcitabine. *Science* **2017**, *357*, 1156−1160.

(14) Bhatt, A. P.; Redinbo, M. R.; Bultman, S. J. The role of the microbiome in cancer development and therapy. *Ca-Cancer J. Clin.* **2017**, *67*, 326−344.

(15) Gunjur, A. Cancer and the microbiome. *Lancet Oncol.* **2020**, *21*, P888.

(16) Fu, A.; Yao, B.; Dong, T.; Chen, Y.; Yao, J.; Liu, Y.; Li, H.; Bai, H.; Liu, X.; Zhang, Y.; Wang, C.; Guo, Y.; Li, N.; Cai, S. Tumor-resident intracellular microbiota promotes metastatic colonization in breast cancer. *Cell* **2022**, *185*, 1356−1372.e26.

(17) Thompson, K. J.; Ingle, J. N.; Tang, X.; Chia, N.; Jeraldo, P. R.; Walther-Antonio, M. R.; Kandimalla, K. K.; Johnson, S.; Yao, J. Z.; Harrington, S. C. A comprehensive analysis of breast cancer microbiota and host gene expression. *PLoS One* **2017**, *12*, No. e0188873.

(18) Banerjee, S.; Tian, T.; Wei, Z.; Shih, N.; Feldman, M. D.; Peck, K. N.; DeMichele, A. M.; Alwine, J. C.; Robertson, E. S. Distinct microbial signatures associated with different breast cancer types. *Front. Microbiol.* **2018**, *9*, 951.

(19) Greathouse, K. L.; White, J. R.; Vargas, A. J.; Bliskovsky, V. V.; Beck, J. A.; von Muhlinen, N.; Polley, E. C.; Bowman, E. D.; Khan, M. A.; Robles, A. I. Interaction between the microbiome and TP53 in human lung cancer. *Genome Biol.* **2018**, *19*, 123.

(20) Gao, Z.; Guo, B.; Gao, R.; Zhu, Q.; Qin, H. Microbiota disbiosis is associated with colorectal cancer. *Front. Microbiol.* **2015**, *6*, 20.

(21) Sfanos, K. S.; Sauvageot, J.; Fedor, H. L.; Dick, J. D.; De Marzo, A. M.; Isaacs, W. B. A molecular analysis of prokaryotic and viral DNA sequences in prostate tissue from patients with prostate cancer indicates the presence of multiple and diverse microorganisms. *Prostate* **2008**, *68*, 306−320.

(22) Poore, G. D.; Kopylova, E.; Zhu, Q.; Carpenter, C.; Fraraccio, S.; Wandro, S.; Kosciolek, T.; Janssen, S.; Metcalf, J.; Song, S. J. Microbiome analyses of blood and tissues suggest cancer diagnostic approach. *Nature* **2020**, *579*, 567−574.

(23) Nejman, D.; Livyatan, I.; Fuks, G.; Gavert, N.; Zwang, Y.; Geller, L. T.; Rotter-Maskowitz, A.; Weiser, R.; Mallel, G.; Gigi, E. The human

tumor microbiome is composed of tumor type−specific intracellular bacteria. *Science* **2020**, *368*, 973−980.
(24) McPherson, A. C.; Pandey, S. P.; Bender, M. J.; Meisel, M. Systemic immunoregulatory consequences of gut commensal translocation. *Trends Immunol.* **2021**, *42*, 137−150.
(25) Bertocchi, A.; Carloni, S.; Ravenda, P. S.; Bertalot, G.; Spadoni, I.; Lo Cascio, A. L.; Gandini, S.; Lizier, M.; Braga, D.; Asnicar, F. Gut vascular barrier impairment leads to intestinal bacteria dissemination and colorectal cancer metastasis to liver. *Cancer Cell* **2021**, *39*, 708−724.e11.
(26) Sommariva, M.; Le Noci, V.; Bianchi, F.; Camelliti, S.; Balsari, A.; Tagliabue, E.; Sfondrini, L. The lung microbiota: role in maintaining pulmonary immune homeostasis and its implications in cancer development and therapy. *Cell. Mol. Life Sci.* **2020**, *77*, 2739−2749.
(27) Blaustein, R. A.; Seed, P. C.; Hartmann, E. M. Biotransformation of Doxorubicin Promotes Resilience in Simplified Intestinal Microbial Communities. *mSphere* **2021**, *6*, No. e0006821.
(28) Hui, Y. F.; Reitz, J. Gemcitabine: a cytidine analogue active against solid tumors. *Am. J. Health-Syst. Pharm.* **1997**, *54*, 162−170.
(29) Hertel, L. W.; Boder, G. B.; Kroin, J. S.; Rinzel, S. M.; Poore, G. A.; Todd, G. C.; Grindey, G. B. Evaluation of the antitumor activity of gemcitabine (2′, 2′-difluoro-2′-deoxycytidine). *Cancer Res.* **1990**, *50*, 4417−4422.
(30) Braakhuis, B.; van Haperen, V. R.; Welters, M.; Peters, G. Schedule-dependent therapeutic efficacy of the combination of gemcitabine and cisplatin in head and neck cancer xenografts. *Eur. J. Cancer* **1995**, *31*, 2335−2340.
(31) Merriman, R. L.; Hertel, L. W.; Schultz, R. M.; Houghton, P. J.; Grindey, G. B. Comparison of the antitumor activity of gemcitabine and ara-C in a panel of human breast, colon, lung and pancreatic xenograft models. *Invest. New Drugs* **1996**, *14*, 243−247.
(32) Manegold, C. Gemcitabine (Gemzar) in non-small cell lung cancer. *Expert Rev. Anticancer Ther.* **2004**, *4*, 345−360.
(33) Heinemann, V. Gemcitabine in metastatic breast cancer. *Expert Rev. Anti-Infect. Ther.* **2005**, *5*, 429−443.
(34) Abbruzzese, J. L.; Grunewald, R.; Weeks, E.; Gravel, D.; Adams, T.; Nowak, B.; Mineishi, S.; Tarassoff, P.; Satterlee, W.; Raber, M. A phase I clinical, plasma, and cellular pharmacology study of gemcitabine. *J. Clin. Oncol.* **1991**, *9*, 491−498.
(35) Han, H.; Li, S.; Zhong, Y.; Huang, Y.; Wang, K.; Jin, Q.; Ji, J.; Yao, K. Emerging pro-drug and nano-drug strategies for gemcitabine-based cancer therapy. *Asian J. Pharm. Sci.* **2022**, *17*, 35−52.
(36) Xi, J.; Wang, Y.; Gao, X.; Huang, Y.; Chen, J.; Chen, Y.; Fan, L.; Gao, L. Reverse intratumor bacteria-induced gemcitabine resistance with carbon nanozymes for enhanced tumor catalytic-chemo therapy. *Nano Today* **2022**, *43*, 101395.
(37) Yang, X.; Qiu, Q.; Liu, G.; Ren, H.; Wang, X.; Lovell, J. F.; Zhang, Y. Traceless antibiotic-crosslinked micelles for rapid clearance of intracellular bacteria. *J. Controlled Release* **2022**, *341*, 329−340.
(38) Zhang, Y.; Wang, D.; Goel, S.; Sun, B.; Chitgupi, U.; Geng, J.; Sun, H.; Barnhart, T. E.; Cai, W.; Xia, J. Surfactant-stripped frozen pheophytin micelles for multimodal gut imaging. *Adv. Mater.* **2016**, *28*, 8524−8530.
(39) Sies, H. Glutathione and its role in cellular functions. *Free Radicals Biol. Med.* **1999**, *27*, 916−921.
(40) Liu, G.; Jiang, Z.; Lovell, J. F.; Zhang, L.; Zhang, Y. Design of a Thiol-Responsive, Traceless Prodrug with Rapid Self-Immolation for Cancer Chemotherapy. *ACS Appl. Bio Mater.* **2021**, *4*, 4982−4989.
(41) Ren, H.; Li, J.; Liu, G.; Sun, Y.; Yang, X.; Jiang, Z.; Zhang, J.; Lovell, J. F.; Zhang, Y. Anticancer Vaccination with Immunogenic Micelles That Capture and Release Pristine CD8+ T-Cell Epitopes and Adjuvants. *ACS Appl. Mater. Interfaces* **2022**, *14*, 2510−2521.
(42) Yang, X.; Ren, H.; Zhang, H.; Liu, G.; Jiang, Z.; Qiu, Q.; Yu, C.; Murthy, N.; Zhao, K.; Lovell, J. F. Antibiotic cross-linked micelles with reduced toxicity for multidrug-resistant bacterial sepsis treatment. *ACS Appl. Mater. Interfaces* **2021**, *13*, 9630−9642.

https://doi.org/10.1021/acs.bioconjchem.2c00407
Bioconjugate Chem. 2022, 33, 1944−1952